

Article

An Insight to the Outage Performance of Multi-Hop Mixed RF/FSO/UWOC System

Hala H. Alhashim ¹, Abdulilah Mohammad Mayet ², Neeraj Kumar Shukla ², Shilpi Birla ³, Mona Aggarwal ⁴, Anshul Vats ⁵, Hemani Kaushal ^{6,*}, Piyush Kuchhal ⁷, Ramy Mohammed Aiesh Qaisi ⁸, Pooja Sabherwal ⁴ and Mohammed Abdul Muqet ²

- ¹ Department of Physics, College of Science, Imam Abdulrahman Bin Faisal University, Dammam 31441, Saudi Arabia; halhashim@iau.edu.sa
- ² Electrical Engineering Department, College of Engineering, King Khalid University, Abha 61411, Saudi Arabia; amayet@kku.edu.sa (A.M.M.); nshukla@kku.edu.sa (N.K.S.); mabdulmuqet@kku.edu.sa (M.A.M.)
- ³ Department of ECE, Manipal University Jaipur, Jaipur 303007, India; shilpi.birla@jaipur.manipal.edu
- ⁴ Department of MDE, North Cap University, Sector 23 A, Gurgaon 122017, India; monaaggarwal@ncuindia.edu (M.A.); pooja@ncuindia.edu (P.S.)
- ⁵ Project Engineer Level-2 in ERNET India, Ministry of Electronics and Information Technology, Government of India, New Delhi 411008, India; anshul@ernet.in
- ⁶ Electrical Engineering Department, University of North Florida, Jacksonville, FL 32224, USA
- ⁷ Department of Electrical and Electronics Engineering, School of Advanced Engineering, UPES, Dehradun 248007, India; pkuchhal@ddn.upes.ac.in
- ⁸ Department of Electrical and Electronics Engineering, College of Engineering, University of Jeddah, Jeddah 21589, Saudi Arabia; dgaisi@uj.edu.sa
- * Correspondence: hemani.kaushal@unf.edu

Abstract: In this paper, we investigate the outage performance of the three-hop mixed system integrating radio frequency (RF), free space optics (FSO), and under water optical communication (UWOC) system. The closed-form analytical expressions for the outage probability of the system are derived. In the considered system, the RF channel follows the Nakagami- m distribution, the FSO channel observes the Gamma-Gamma fading statistics, and the UWOC link experiences a mixture Exponential Generalized Gamma (EGG) fading distribution. To verify the derived analytical expressions, numerical simulations are also carried out, and we present the influence of the various link parameters such as path loss, atmospheric turbulence, pointing errors, angle-of-arrival fluctuations, water salinity, and scintillation on the performance of the decode and forward (DF) relayed multi-hop communication system.

Keywords: asymptotic outage probability; Gamma-Gamma distribution; exponential generalized gamma fading; Nakagami- m fading



Citation: Alhashim, H.H.; Mayet, A.M.; Shukla, N.K.; Birla, S.; Aggarwal, M.; Vats, A.; Kaushal, H.; Kuchhal, P.; Qaisi, R.M.A.; Sabherwal, P.; et al. An Insight to the Outage Performance of Multi-Hop Mixed RF/FSO/UWOC System. *Photonics* **2023**, *10*, 1010. <https://doi.org/10.3390/photonics10091010>

Received: 12 June 2023

Revised: 17 August 2023

Accepted: 18 August 2023

Published: 4 September 2023



Copyright: © 2023 by the authors. Licensee MDPI, Basel, Switzerland. This article is an open access article distributed under the terms and conditions of the Creative Commons Attribution (CC BY) license (<https://creativecommons.org/licenses/by/4.0/>).

1. Introduction

The free space optical (FSO) network has become a competent point-to-point wireless transmission solution because of the availability of its high bandwidth in the unregulated spectrum [1]. When the FSO networks are compared with their counterpart radio frequency (RF) systems, they offer much higher bandwidth and capacity. In wireless communication systems, the FSO provides a favorable solution for last mile connectivity issues. It is suitable for a wide range of applications like the back-haul of cellular systems, enterprise/building connectivity, disaster recovery redundant backup links, etc. [2]. The FSO systems need a direct line-of-sight (LOS) path and their transmission is tremendously controlled by the atmospheric turbulence and the pointing error; hence, these factors affect the performance of FSO systems [3–7]. To combine the benefits of both lines, mixed networks that include both RF and FSO links have been recommended. While the RF link is a great complement

to the FSO channel because it is relatively unresponsive to the weather and can easily pass through the fog, the FSO link offers much higher data rates than the RF link, but suffers from atmospheric loss due to the fog and scintillation [8].

The hybrid RF/FSO system can be viewed as a way to lessen the effects of turbulence in the atmosphere and pointing errors [9]. In mixed RF/FSO communication networks, the relays play a significant role in transferring the information signal from the source node to the destination. The study and performance evaluation of mixed RF/FSO systems has been carried out extensively in the literature. The performance of amplify and forward (AF) relay-based mixed RF/FSO systems is presented in [10–13] considering intensity modulation/direct detection (IM/DD) and heterodyne modulation schemes. The decode and forward (DF) relay-based mixed RF/FSO systems are studied in [14–16]. The author in [17] considered a unmanned aerial vehicle (UAV)-assisted RF/FSO system and obtained the expression for the outage probability (OP) and the optimal altitude. In [18], the authors analyzed the performance of the UAV-based RF/FSO communication system by evaluating its asymptotic average secrecy rate.

In recent years, optical signals have also gained a lot of attention in underwater wireless communication because of their various advantages like wider bandwidth, higher data transmission rate, etc., and hence they provide an efficient transmission solution for a variety of underwater applications [19] such as military defense, port security, seismic monitoring, etc. Underwater wireless optical communication (UWOC) is an emerging field of research nowadays. Due to the difficult communication features, exploring the deep environment is a challenging endeavor. The high data transfer rate of collected data to control stations is another challenge in ocean monitoring applications. Each individual RF, FSO, and UWOC system has its own drawbacks and difficulties. Therefore, the mixed system helps to provide better exploration, monitoring, and transmission of the ocean data between the source and the destination. There has been rapid growth in the implementation of mixed RF/FSO/UWOC systems over the past few years, because the mixed systems are able to fulfill the data bandwidth requirement and provide easy data transmission from the source to the destination under different fading conditions. It has become interesting to combine RF communication with optical wireless communication (including FSO communication and UWOC).

The authors in [20] explored the performance of the relay-based mixed RF/UWOC system where the relay conveys the information to an autonomous underwater vehicle (AUV) which is acting as the destination. The DF relay-based dual-hop mixed RF/UWOC is proposed in [21] and the author derived the novel expressions of the average bit error rate (ABER) for the different modulation schemes. In [22], the author put forth a dual-hop mixed RF/UWOC system based on UAVs and generated innovative expressions for OP and ABER of the system. The cooperative AF relay-based system is proposed and the outage analysis of the same is presented by the author in [23]. In [24], the authors have derived the closed-form expressions for the OP and ABER for both AF and DF relay-based mixed RF/UWOC systems. In [25], the asymptotic outage analysis and the secrecy outage performance analysis is carried out for a dual-hop RF/UWOC system. The authors in [26] have considered a DF relayed three-hop RF/FSO/UWOC system and evaluated the outage and error performance of the system. The RF, FSO, and UWOC links are modeled by Nakagami- m distribution, Double Generalized Gamma (DGG) distributed fading, and Rayleigh distributed pointing errors and Exponential Generalized Gamma (EGG) distribution, respectively. However, the mathematical modeling of the ABER of the proposed system is not tractable, and thus not easy to understand. Motivated by the above advantages of the mixed communication systems (RF systems and optical systems), we propose in this paper a DF relay-based three-hop RF/FSO/UWOC system.

Contributions

We present a three-hop mixed RF/FSO/UWOC system where the RF link, FSO link, and UWOC link are modeled by Nakagami- m fading distribution, Gamma-Gamma distri-

bution under the influence of pointing errors, and Exponential Generalized Gamma (EGG) distribution, respectively. The first relay node receives information from the source node located at a distance via RF link. The first intermediate DF relay node then transmits the signal towards the second intermediate DF relay node via FSO link. Furthermore, the second relay node decodes and forwards the received signal towards the destination receiver on the UWOC link. To investigate the performance of the proposed three-hop mixed system model, the SNR statistics of the considered multi-hop system are derived in terms of the cumulative distribution function (CDF) of the end-to-end instantaneous signal-to-noise ratio (SNR) of the system. Later, these statistics are utilized to derive the closed-form analytical expression for the system outage probability. The proposed mixed system’s behavior under high-SNR conditions is monitored. Additionally, numerical simulation is used to confirm the mathematical analysis of the suggested model while taking into account the influence of different link factors, such as the effect of path loss, atmospheric turbulence, pointing errors, angle-of-arrival (AOA) fluctuations, multipath fading parameter, water salinity, scintillation caused by air bubbles, and temperature gradient.

The proposed three-hop communication system model and channel models of RF, FSO, and UWOC links are presented in Section 2. The outage probability analysis of the proposed system and asymptotic outage analysis are carried out in Sections 3 and 4, respectively. The simulation results and numerical results are demonstrated in Section 5, and lastly, the paper is concluded in Section 6. For ease of reference a list of abbreviations and symbols utilized in the paper are given in Table 1 and Table 2, respectively.

Table 1. List of abbreviations.

1.	RF	Radio frequency
2.	FSO	Free space optics
3.	UWOC	Underwater optical communication
4.	EGG	Exponential generalized gamma
5.	DF	Decode and forward
6.	AF	Amplify and forward
7.	LOS	Line-of-sight
8.	IM/DD	Intensity modulation/direct detection
9.	UAV	Unmanned aerial vehicle
10.	AUV	Autonomous underwater vehicle
11.	ABER	Average bit error rate
12.	OP	Outage probability
13.	CDF	Cumulative distribution function
14.	PDF	Probability density function
15.	SNR	Signal-to-noise ratio
16.	AOA	Angle-of-arrival

Table 2. List of symbols.

1.	R_1, R_2	Relay 1, Relay 2
2.	θ_{FOV}	Angle-of-arrival fluctuations
3.	$F_{\gamma_{RF}}(\gamma)$	CDF of SNR of RF link
4.	$f_{\gamma_{RF}}(\gamma)$	PDF of SNR of RF link

Table 2. *Cont.*

5.	$\bar{\gamma}_{RF}$	Average SNR of RF link
6.	γ	Instantaneous SNR of the RF/FSO/UWOC link
7.	$\Gamma(\cdot, \cdot)$	Upper incomplete Gamma function
8.	L_{RF}	RF channel path loss
9.	α	Path loss exponent
10.	A	Constant related to the transmission environment and frequency of the RF information signal
11.	d_{RF}	Distance between source and relay 1
12.	m	Nakagami-m fading parameter
13.	K	Rician factor
14.	$\bar{\gamma}_{FSO}$	Average SNR of FSO link
15.	ρ	Optical-to-electrical efficiency
16.	P_{t_1}	Source transmitted optical power
17.	σ_{n_1}	Standard deviation of Gaussian noise
18.	σ_{θ}^2	Variance of Tx–Rx misalignment orientations
19.	ζ	Pointing error in FSO link
20.	σ_s	Standard deviation of the pointing error displacement
21.	w_e	Equivalent beam width at the receiver
22.	α_f, β_f	Atmospheric turbulence parameters
23.	$\Gamma(\cdot)$	Standard Gamma function
24.	$erf(\cdot)$	Error function
25.	h_l	Atmospheric path loss
26.	$F_{\gamma_{FSO}}(\gamma)$	CDF of SNR of FSO link
27.	$f_{\gamma_{FSO}}(\gamma)$	PDF of SNR of FSO link
28.	$F_{\gamma_{UW}}(\gamma)$	CDF of SNR of UWOC link
29.	$f_{\gamma_{UW}}(\gamma)$	PDF of SNR of UWOC link
30.	r	Constant for modulation and detection technique
31.	μ_r	Average SNR of the UWOC link
32.	w, λ, a, b, c	Parameters associated with the EGG distribution of the UWOC link
32.	γ_{DF}	SNR of the received signal at destination node
33.	$\gamma_{RF}, \gamma_{FSO}, \gamma_{UW}$	Instantaneous SNR of the RF, FSO and UWOC links resp.
34.	$F_{\gamma_{DF}}(\gamma)$	CDF of the end-to-end source to destination link
35.	γ_{th}	Threshold SNR
36.	$P_{out}^{DF}(\gamma_{th})$	Outage probability of the system
37.	P_{out}	Outage probability of the system at high-SNR region
38.	G_C^{xy}	Coding gain
39.	G_D^{xy}	Diversity gain
40.	d_{FSO}	FSO link distance

2. System Modeling

The system model demonstrated in Figure 1 presents a three-hop mixed RF/FSO/UWOC system employing DF relaying protocol. In the proposed model, the source node shown by S sends the information signal towards the destination node denoted as D . We assume that no direct communication is feasible between the source and the destination nodes due to different environmental obstacles and long distance; hence, communication between these two takes place with the help of two DF relays, termed R_1 and R_2 . The source S is situated at the distant location and sends the signaling information towards the destination node D , such as ocean divers. The S in the first hop sends the information signal towards the first relay R_1 , which is mounted on the lighthouse. This link (SR_1) is assumed to be an RF link. The received information signal at R_1 is decoded and converted into the FSO signal and forwarded towards the second relay, R_2 , which is mounted on a floating vehicle (FV) over the sea surface, such as a boat used by the ocean divers. The second relay, R_2 , decodes the received FSO signal, converts it to a visible light signal, and forwards the optical signal to the divers under the sea surface via UWOC link. Here, the Doppler effect is ignored and the UWOC link is assumed to be static.

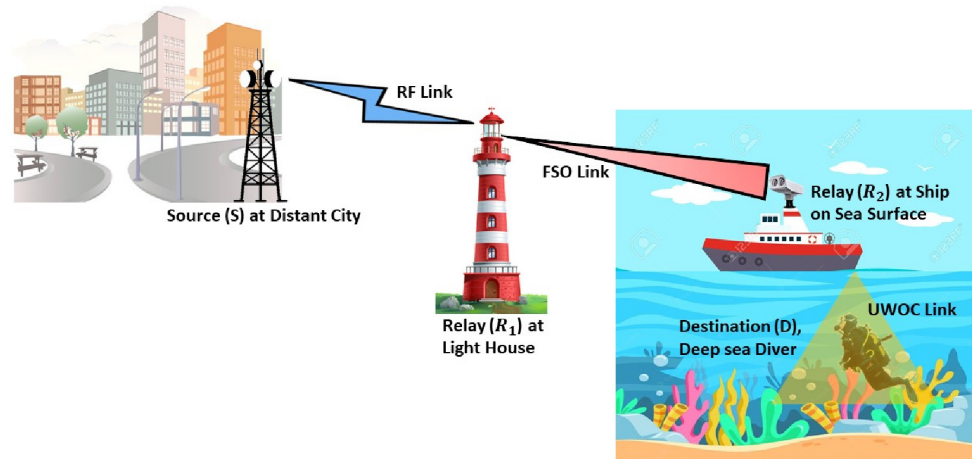


Figure 1. Three-hop mixed RF/FSO/UWOC system.

For the presented three-hop mixed system, the RF link is assumed to be modeled by Nakagami- m distribution, the FSO channel is modeled by the Gamma-Gamma fading statistics considering the impact of pointing errors, atmospheric turbulence, and angle-of-arrival (AOA) fluctuations, denoted as θ_{FOV} , and the UWOC link is assumed to be modeled by EGG distribution, respectively. It has been assumed that the optical signal transmission underwater is remarkably influenced by absorption and scattering, rather than the turbulence caused by the temperature gradient and air bubbles under the water.

2.1. RF Link Modeling

The Nakagami- m channel model is a generalized model and mathematically tractable [20]. Here in this section, we deal with the detailed description of the RF link modeling. At R_1 , the CDF of the instantaneous SNR, $F_{\gamma_{RF}}(\gamma)$, is given by Equation (2), as in [27], as

$$F_{\gamma_{RF}}(\gamma) = 1 - \frac{1}{\Gamma(m)} \Gamma\left(m, \frac{mL_{RF}\gamma}{\bar{\gamma}_{RF}}\right) \quad (1)$$

where $\bar{\gamma}_{RF}$ represents the average SNR, γ is the instantaneous SNR of the RF link, $\Gamma(\dots)$ stands for the upper incomplete Gamma function, L_{RF} is the RF channel path loss given as $L_{RF} = Ad_{RF}^\alpha$, where α represents the path loss exponent, A is assumed to be a constant related to the transmission environment and frequency of the information signal, and d_{RF} represents the distance between S and R_1 . The parameter m denotes the Nakagami- m

fading parameter and it can be calculated as $m \approx \frac{(K+1)^2}{2K+1}$; K here stands for the Rician factor [28].

2.2. FSO Link

The FSO link follows the Gamma-Gamma fading statistics with the impact of the angle-of-arrival of the FSO beam. The Gamma-Gamma fading model is a general and mathematically tractable composite FSO model [4]. The probability density function (PDF) of instantaneous electrical SNR, $f_{\gamma_{FSO}}(\gamma)$, is given, as in [29,30], as

$$f_{\gamma_{FSO}}(\gamma) = \exp\left(-\frac{\theta_{FOV}^2}{2\sigma_\theta^2}\right) + \left[1 - \exp\left(-\frac{\theta_{FOV}^2}{2\sigma_\theta^2}\right)\right] \times \left[\frac{\zeta^2 \gamma_T^{-1}}{2\Gamma(\alpha_f)\Gamma(\beta_f)} \times G_{1,3}^{3,0}\left(\frac{\alpha_f \beta_f}{A_o h_l} \left(\sqrt{\frac{\gamma}{\tilde{\gamma}_{FSO}}}\right) \middle| \frac{1 + \zeta^2}{\zeta^2, \alpha, \beta}\right)\right], \tag{2}$$

where $\tilde{\gamma}_{FSO} = \frac{(\rho^2 P_{t_1}^2)}{\sigma_{n_1}^2}$, ρ is optical-to-electrical efficiency, P_{t_1} is source-transmitted optical power, σ_{n_1} is the standard deviation of Gaussian noise, σ_θ^2 is the variance of $T_x - R_x$ misalignment orientations, and pointing error $\zeta = \frac{w_e}{2\sigma_s}$; here σ_s stands for the standard deviation of the pointing error displacement, and w_e is the equivalent beam width at the receiver. α_f and β_f represent the atmospheric turbulence parameters associated with the atmospheric conditions and $\Gamma(\cdot)$ stands for the standard Gamma function. $A_o = erf^2(v)$, where $erf(\cdot)$ denotes the error function and h_l stands for atmospheric path loss, given as in [31]. Now integrating (2) using ([Equation (07.34.21.0084.01) [32]), we derive the closed-form expression for the CDF of instantaneous SNR for the FSO link given as

$$F_{\gamma_{FSO}}(\gamma) = \exp\left(-\frac{\theta_{FOV}^2}{2\sigma_\theta^2}\right) + \left[1 - \exp\left(-\frac{\theta_{FOV}^2}{2\sigma_\theta^2}\right)\right] \times \left[\frac{\zeta^2}{\Gamma(\alpha_f)\Gamma(\beta_f)} \times G_{2,4}^{3,1}\left(\frac{\alpha_f \beta_f}{A_o h_l} \left(\sqrt{\frac{\gamma}{\tilde{\gamma}_{FSO}}}\right) \middle| \zeta^2, \alpha, \beta, 0\right)\right]. \tag{3}$$

2.3. UWOC Link Modeling

This section deals with UWOC link modeling. It has been assumed that the optical signal transmission underwater is remarkably influenced by absorption and scattering, rather than the turbulence caused by the temperature gradient and air bubbles under the water. The combined effect of the fading can be appropriately characterized by the Exponential Generalized Gamma distribution with different water salinity. The CDF of the instantaneous SNR, $F_{\gamma_{UW}}(\gamma)$, of the UWOC link is given by Equation (21) in [33] as

$$F_{\gamma_{UW}}(\gamma) = w G_{1,2}^{1,1}\left(\frac{1}{\lambda} \left(\frac{\gamma}{\mu_r}\right)^{\frac{1}{r}} \middle| \frac{1}{1, 0}\right) + \frac{1-w}{\Gamma(a)} G_{1,2}^{1,1}\left(\frac{1}{b^c} \left(\frac{\gamma}{\mu_r}\right)^{\frac{c}{r}} \middle| \frac{1}{a, 0}\right), \tag{4}$$

where w, λ, a, b, c are the parameters associated with the EGG distribution, r is set to 2, which specifies the intensity modulation and direct detection (IM/DD) scheme, and μ_r is the average SNR of the UWOC link. The parameters employed for different water salinity and the temperature gradient for varying bubble levels are taken from [33].

3. Outage Probability Analysis

The outage probability performance of the proposed mixed multihop communication system is investigated in this section. For the proposed system, the end-to-end instantaneous SNR of the received signal at node D , γ_{DF} , is given as [34]

$$\gamma_{DF} = \min[\gamma_{RF}, \gamma_{FSO}, \gamma_{UW}], \tag{5}$$

where, $\gamma_{FSO}, \gamma_{RF}, \gamma_{UW}$ represent the instantaneous SNRs of FSO, RF, and UWOC links, respectively. Using (5), the equivalent CDF of the γ_{DF} can be written, as given in [35], as

$$F_{\gamma DF}(\gamma) = 1 - (1 - F_{\gamma RF}(\gamma))(1 - F_{\gamma FSO}(\gamma))(1 - F_{\gamma UW}(\gamma)). \tag{6}$$

Further, the probability of the outage can be an important tool in evaluating the reliability of the communication systems. It can be defined as the probability when γ_{DF} is lower than the specific value of the threshold, γ_{th} such that the system performance is considered as insufficient. Accordingly, the P_{out}^{DF} may be evaluated from (6) by substituting γ by γ_{th} , that is, $P_{out}^{DF}(\gamma_{th}) = F_{\gamma DF}(\gamma_{th})$. Therefore, substituting $F_{\gamma RF}(\gamma)$, $F_{\gamma FSO}(\gamma)$, and $F_{\gamma UW}(\gamma)$ from (1), (3), and (4), respectively, and putting γ_{th} in place of γ , we obtain the closed-form expression for the probability of outage of the proposed mixed RF/FSO/UWOC system, shown as

$$\begin{aligned}
 P_{out}^{DF} = & 1 - \left[\left[1 - \frac{1}{\Gamma(m)} \Gamma\left(m, \frac{mL_{RF}\gamma_{th}}{\tilde{\gamma}_{RF}}\right) \right] \right. \\
 & \times \left[1 - wG_{1,2}^{1,1}\left(\frac{1}{\lambda}\left(\frac{\gamma_{th}}{\mu_r}\right)^{\frac{1}{r}} \mid 1, 0\right) - \frac{1-w}{\Gamma(a)} G_{1,2}^{1,1}\left(\frac{1}{b^c}\left(\frac{\gamma_{th}}{\mu_r}\right)^{\frac{c}{r}} \mid a, 0\right) \right] \\
 & \times \left[1 - \exp\left(-\frac{\theta_{FOV}^2}{2\sigma_\theta^2}\right) - \left(1 - \exp\left(-\frac{\theta_{FOV}^2}{2\sigma_\theta^2}\right)\right) \right. \\
 & \left. \left. \times \left(\frac{\zeta^2}{\Gamma(\alpha_f)\Gamma(\beta_f)} G_{2,4}^{3,1}\left(\frac{\alpha_f\beta_f}{A_o h_l}\left(\sqrt{\frac{\gamma_{th}}{\tilde{\gamma}_{FSO}}}\right) \mid 1, 1 + \zeta^2\right)\right) \right] \right]. \tag{7}
 \end{aligned}$$

4. Asymptotic Analysis

The analytical expression for the outage probability of the considered system model is quite complex. Therefore, asymptotic outage probability provides more understanding on the impact of the system’s channel parameters on the system’s outage probability. By assuming an independent and identically distributed case, that is, $\tilde{\gamma}_{RF} = \tilde{\gamma}_{FSO} = \tilde{\gamma}_{UW}$, the overall asymptotic outage probability can be written as the sum of the individual asymptotic CDF of the each channel SNR. In the high-SNR region, the overall asymptotic outage performance of the triple-hop mixed communication system can be approximated as

$$P_{out}^\infty \cong F_{\gamma DF}^\infty(\gamma_{th}) \cong F_{\gamma RF}^\infty(\gamma_{th}) + F_{\gamma FSO}^\infty(\gamma_{th}) + F_{\gamma UW}^\infty(\gamma_{th}), \tag{8}$$

where $F_{\gamma RF}^\infty(\gamma_{th})$, $F_{\gamma FSO}^\infty(\gamma_{th})$, and $F_{\gamma UW}^\infty(\gamma_{th})$ are CDF’s of $S \rightarrow R_1$, $R_1 \rightarrow R_2$, and $R_2 \rightarrow D$ links at high-SNR regimes, respectively.

The coding gain and the diversity order can be defined as $(G_C^{xy}\tilde{\gamma})^{-G_D^{xy}}$, where $xy \in \{SR_1, R_1R_2, R_1D\}$, G_C^{xy} is the coding gain and G_D^{xy} is the diversity order of the link [36]. We need to find out $F_{\gamma RF}^\infty(\gamma_{th})$, $F_{\gamma FSO}^\infty(\gamma_{th})$, and $F_{\gamma UW}^\infty(\gamma_{th})$ one by one as shown below.

4.1. RF Link ($S \rightarrow R_1$)

At high-SNR regime, the CDF of the first hop, i.e., the RF link given in (1), can be re-written according to the form given in [37], as

$$F_{\gamma RF}^\infty(\gamma) = \frac{1}{\Gamma(m+1)} \left(\frac{m\gamma_{th}L_{RF}}{\tilde{\gamma}}\right)^m. \tag{9}$$

4.2. FSO Link ($R_1 \rightarrow R_2$)

At high-SNR regime, the CDF of the FSO link, as given in (3), can be written asymptotically using identity ([38], Equation (6.2.2)) [36], as

$$\begin{aligned}
 F_{\gamma\text{FSO}}^\infty(\gamma) &= A \sum_{k=1}^6 \frac{\prod_{j=1}^6 \Gamma(b_j - b_k) \Gamma(b_k)}{\prod_{j=2}^3 \Gamma(a_j - b_k) \Gamma(1 + b_k)} B^{b_k/2} \left(\frac{\gamma_{th}}{\tilde{\gamma}}\right)^{\frac{b_k}{2}} \\
 &= \left(\frac{X^{\frac{-2}{b_k}}}{\gamma_{th}} \tilde{\gamma}\right)^{\frac{-b_k}{2}},
 \end{aligned}
 \tag{10}$$

where $a_j = a_p(j)$, for $j = 1$ to 3 ,

$$a_1 = 1,$$

$$b_j = b_q(j), j = 1 \text{ to } 6,$$

$$b_7 = 0,$$

$$b_k = \min\{\zeta^2, \alpha, \beta\}.$$

The constant X is equal to $A \sum_{k=1}^6 \frac{\prod_{j=1}^6 \Gamma(b_j - b_k) \Gamma(b_k)}{\prod_{j=2}^3 \Gamma(a_j - b_k) \Gamma(1 + b_k)} B^{b_k/2}$,

$$A = \left[1 - \exp\left(\frac{-\theta_{FOV}^2}{2\sigma_\theta}\right) \times \frac{2^{(\alpha+\beta-2)}}{2\pi\Gamma(\alpha)\Gamma(\beta)}\right],$$

$$B = \left(\frac{(\alpha\beta)^2}{16}\right)^{\frac{b_k}{2}}.$$

4.3. UWOC Link ($R_2 \rightarrow D$)

The asymptotic expression of the CDF of the third hop, i.e., the UWOC link, given in (4), can be expressed as in [39], as

$$F_{\gamma\text{UW}}^\infty(\gamma) \simeq \frac{\omega\gamma_{th}}{\lambda\tilde{\gamma}} + \frac{1 - \omega}{\Gamma(a + 1)} \left(\frac{\gamma_{th}}{b\tilde{\gamma}}\right)^{ac}. \tag{11}$$

Further, substituting (9), (10), and (11) in (8) and re-arranging terms, the asymptotic expression at high-SNR regime for the end-to-end outage probability of the system can be given as

$$\begin{aligned}
 P_{out}^\infty &= \left(\frac{\Gamma(m + 1)^{\frac{1}{m}}}{mL_{RF}\gamma_{th}} \cdot \tilde{\gamma}\right)^{-m} + \left(\frac{X^{\frac{-2}{b_k}}}{\gamma_{th}} \tilde{\gamma}\right)^{\frac{-b_k}{2}} \\
 &\quad + \left(\frac{\lambda}{\omega\gamma_{th}} \cdot \tilde{\gamma}\right)^{-1} + \left(\frac{b\Gamma(a + 1)}{\gamma_{th}(1 - \omega)} \cdot \tilde{\gamma}\right)^{-ac}.
 \end{aligned}
 \tag{12}$$

Now, coding gain and diversity gain are simply evaluated from the asymptotic outage probability of the system mentioned in (12). It can be clearly seen that the system performance is dominated by the parameters of the worst link among the three links. Hence, the diversity gain of the system is $\min(\frac{b_k}{2}, m, ac)$. Based on G_D , there can be three cases to examine the system's overall outage performance, as shown below.

1. Case 1: Among three links, when only one link is dominating, the coding gain can be written as

$$G_C = \begin{cases} \frac{X^{\frac{-2}{b_k}}}{\gamma_{th}}, & G_D = \frac{b_k}{2} \\ \frac{\Gamma(m+1)^{\frac{1}{m}}}{mL_{RF}\gamma_{th}}, & G_D = m \\ \frac{\lambda}{\omega\gamma_{th}} + \frac{b\Gamma(a+1)}{(1-\omega)\gamma_{th}}, & G_D = ac \simeq 1 \end{cases}
 \tag{13}$$

2. Case 2: When two links are dominating out of three links, the coding gain can be written as

$$G_C = \begin{cases} \frac{1}{2} \left(\frac{X^{b_k}}{\gamma_{th}} + \frac{\Gamma(m+1)^{\frac{1}{m}}}{mL_{RF}\gamma} \right), & G_D = \frac{b_k}{2} = m \\ \frac{1}{2} \left(\frac{\Gamma(m+1)^{\frac{1}{m}}}{mL_{RF}\gamma} + \left(\frac{\lambda}{\omega\gamma_{th}} + \frac{b\Gamma(a+1)}{(1-\omega)\gamma_{th}} \right) \right), & G_D = ac \simeq 1 = m \\ \frac{1}{2} \left(\frac{X^{b_k}}{\gamma_{th}} + \left(\frac{\lambda}{\omega\gamma_{th}} + \frac{b\Gamma(a+1)}{(1-\omega)\gamma_{th}} \right) \right), & G_D = ac \simeq 1 = \frac{b_k}{2}. \end{cases} \quad (14)$$

3. Case 3: When all three links are dominating, then the coding gain can be written as

$$G_C = \left\{ \frac{1}{3} \left(\frac{X^{b_k}}{\gamma_{th}} + \frac{\Gamma(m+1)^{\frac{1}{m}}}{mL_{RF}\gamma} + \frac{\lambda}{\omega\gamma_{th}} + \frac{b\Gamma(a+1)}{(1-\omega)\gamma_{th}} \right) \right\}, \quad G_D = \frac{b_k}{2} = m = ac \simeq 1. \quad (15)$$

5. Numerical Results

For the proposed model, the numerical results are plotted for the outage probability at low- and high-SNR regimes for fresh water and salty water in the presence of air bubbles and temperature gradient. We are considering the intensity modulation and direct deduction technique; thus, $r = 2$. The threshold SNR (γ_{th}) is set at 5 dB. The FSO link parameters such as atmospheric attenuation, $h_l = 0.9$, length of the turbulent FSO link, $d_{FSO} = 1$ km, beam radius of the turbulent link, $w_{d_1} = 2.5$ m, the jitter, $\sigma_s = 30$ cm, and turbulence parameters, α_f and β_f , for the FSO link are assumed to be 5.42 and 3.8. Further, the FOV angle of the FSO transceiver at R_2 is 7 mrad and the standard deviation of AOA fluctuations is considered to be $\sigma_\theta = 7$ mrad. The values of considered UWOC link parameters i.e., bubble levels, temperature gradient, w, λ, a, b, c have been adopted from [33].

Figure 2 presents the outage performance of the proposed system under the influence of the AOA fluctuations. It has been demonstrated that the outage performance of the system is not good for the low values of the AoA. However, the outage performance of the system improves significantly with increase in the AOA, θ_{FOV} . For example, at SNR = 25 dB and $\theta_{FOV} = 4$ mrad, the P_{out}^{DF} is equal to 2.499×10^{-3} , and at SNR = 25 dB and $\theta_{FOV} = 8$ mrad, the P_{out}^{DF} is equal to 6.238×10^{-8} . Moreover, it is also noticed that after a certain value of average SNR, the other impairments dominate over AOA fluctuations, and the effect of the AOA fluctuations becomes negligible.

Figure 3 shows the outage performance of the proposed system under varying pointing errors assuming moderately turbulent conditions. It is observed from the plots that the outage probability of the considered system decreases as the value of ζ increases; hence, the system performance increases as pointing errors, parameter ζ , increase. It can be said that the system's performance improves with the decreasing impact of the pointing errors in the FSO channel. The pointing errors result from misalignment between the transmitter and receiver or turbulence.

Figure 4 presents the outage probability of the system w.r.t. the Nakagami fading factor, m with varying average SNR (dB) for the salty water type. It is observed that the system shows high values of outage probability at low values of m (severity is high). The severity decreases as the value of m increases. Further, it is also observed that after a certain value, i.e., $m = 5$, the outage performance of the system becomes stable as the impact of fading due to the RF link becomes negligible. Further, the impact of the fading in the RF link also reduces with an increase in the average SNR of the system. For example, at $m = 5$, SNR = 5 dB, the outage probability is equal to 7.401×10^{-4} and at $m = 5$, SNR = 20 dB, the outage probability is equal to 3.756×10^{-6} .

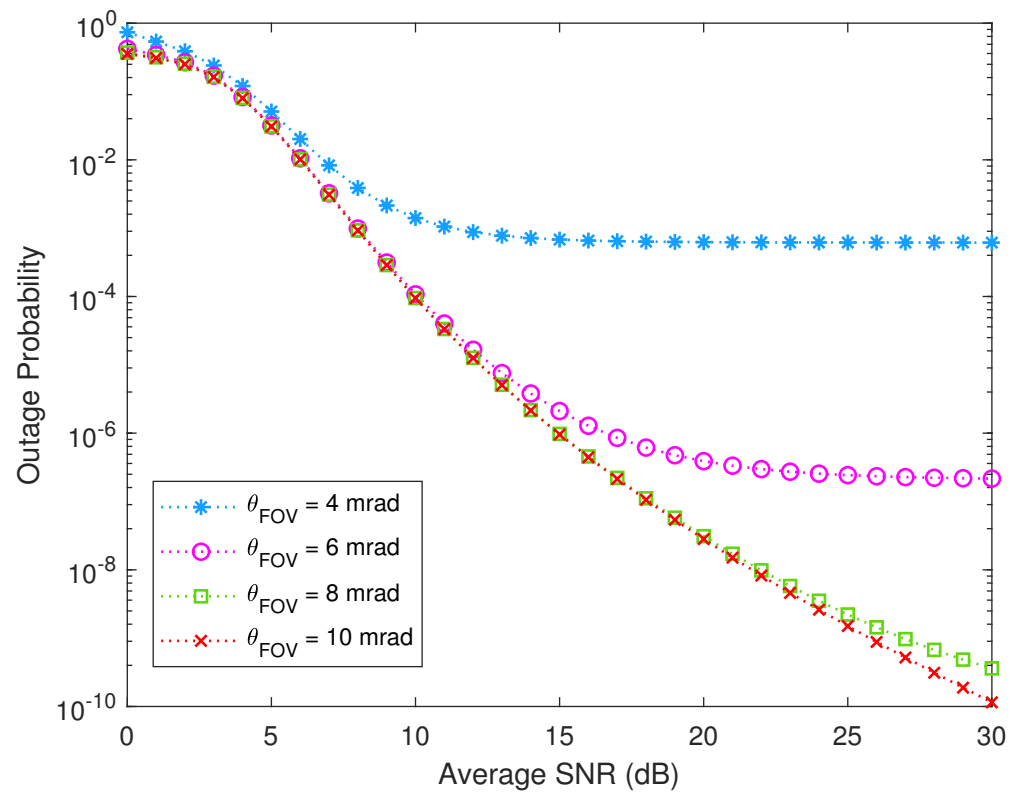


Figure 2. Outage probability variations vs. angle-of-arrival fluctuations.

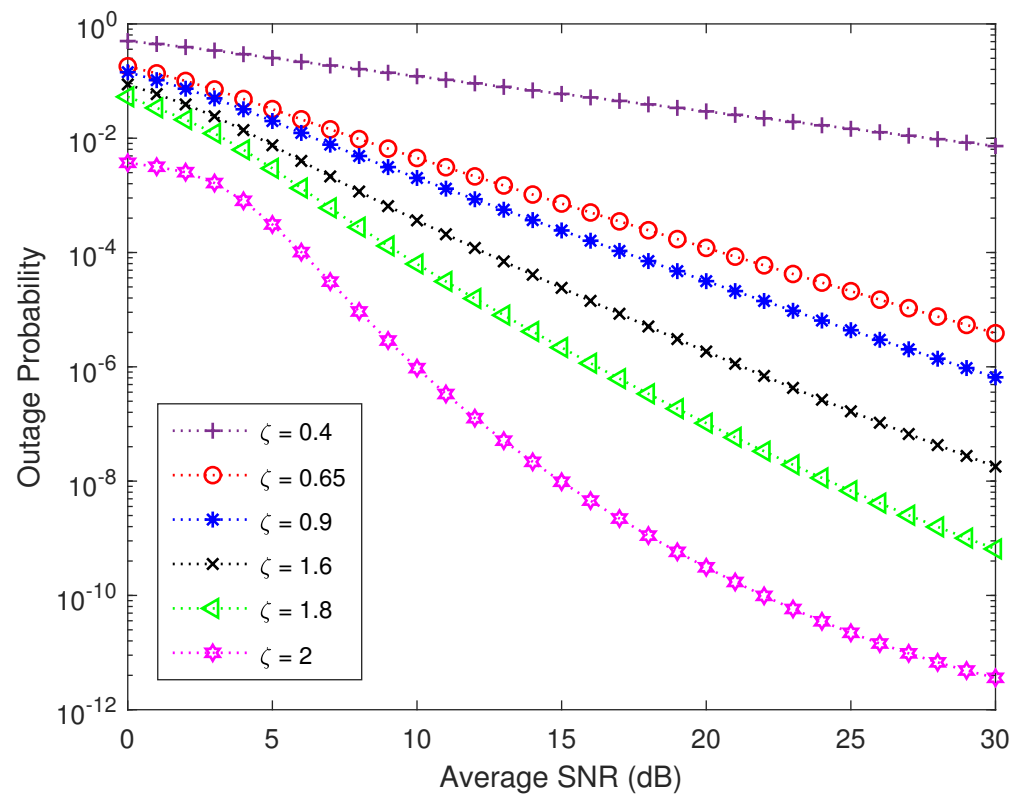


Figure 3. Outage performance of the system with varying pointing errors.

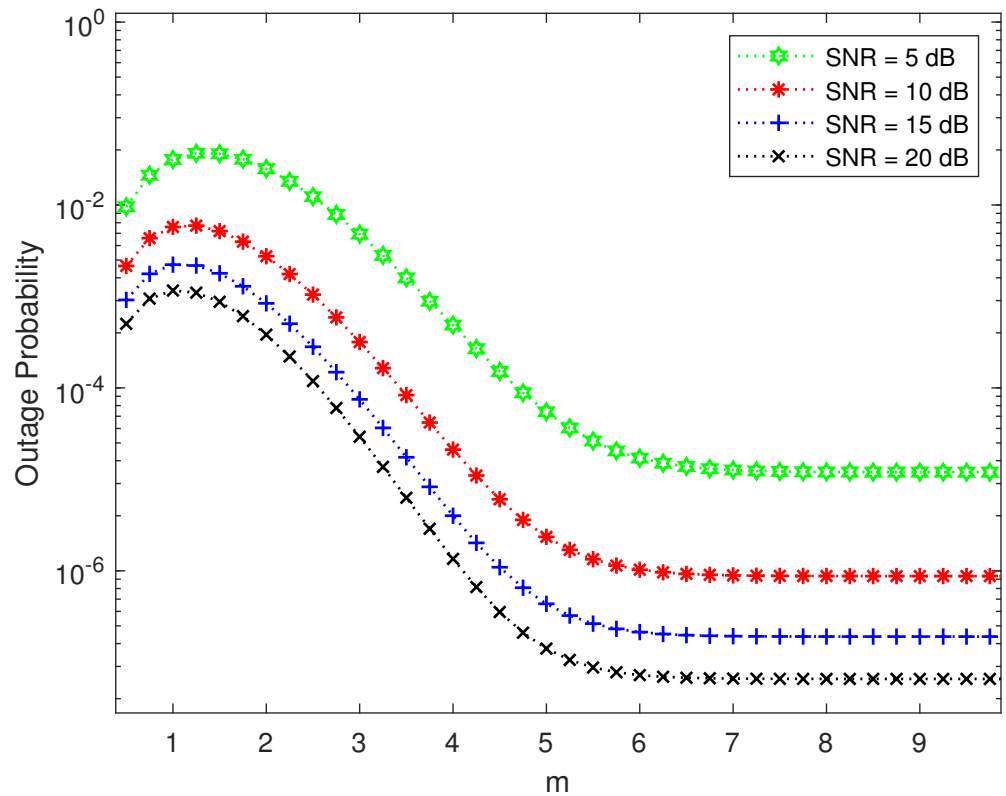


Figure 4. Outage probability vs. average SNR (dB) with variation of Nakagami fading factor m in RF link.

The plot in Figure 5 demonstrates the outage probability of the mixed system under the impact of turbulent water conditions in both water types, i.e., fresh water and salty water types. As expected, the outage performance of the system improves with the decrease in temperature gradient and air bubbles. For example, for fresh water with average SNR at 8 dB and bubble level 4.7 L/min, the P_{out}^{DF} is 2.8836×10^{-6} , and with bubble level 16.5 L/min, the P_{out}^{DF} is 3.4207×10^{-4} . Also, for salty water with average SNR at 8 dB and bubble level 4.7 L/min, the P_{out}^{DF} is 2.2815×10^{-6} , and with bubble level 16.5 L/min, the P_{out}^{DF} is 2.0146×10^{-3} .

Figure 6 shows the outage performance of the system at low-SNR and high-SNR regimes. The graph is plotted for the salty water type and lower bubble level and temperature gradient with pointing error = 2, for moderately turbulent atmospheric conditions with AOA fluctuation = 7 mrad. It is observed that in the simulation results, the asymptotic outage plots are in perfect agreement with the theoretical analysis and the Monte Carlo simulation, hence validating the analytical modeling of the three-hop mixed RF/FSO/UWOC system.

Figure 7 shows the influence of atmospheric turbulence on the outage probability of the system w.r.t. the average SNR in dB at the destination node. We assume direct detection at the receiver with γ_{th} at 0 dB. The outage probability of the system is analyzed in different atmospheric turbulence conditions for $\xi = 2$. The outage probability in highly turbulent conditions is more and it decreases from moderately to weakly turbulent conditions. From the figure it can be seen that the outage probability of the three-hop system reduces as the atmospheric turbulence changes from high- to low-turbulence scenarios. However, for the proposed model, the changes in the outage performance are not significant, and hence the system also slightly outperforms in highly turbulent conditions.

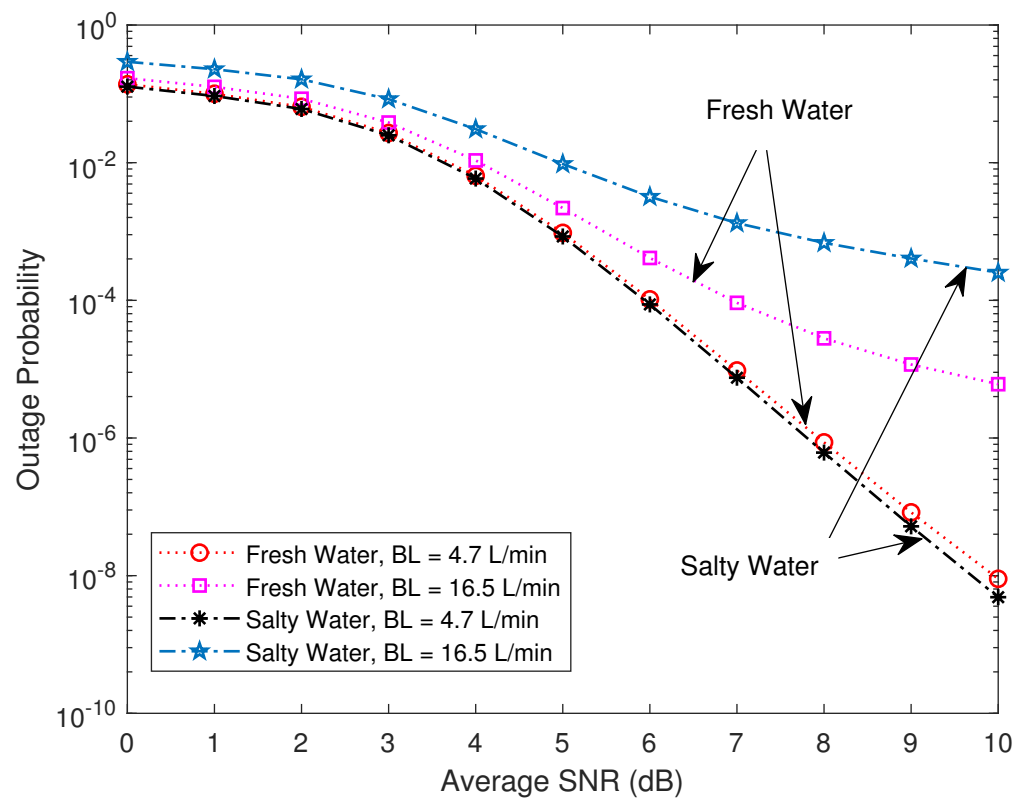


Figure 5. Outage performance of the system under varying bubble levels (BLs) in different water types.

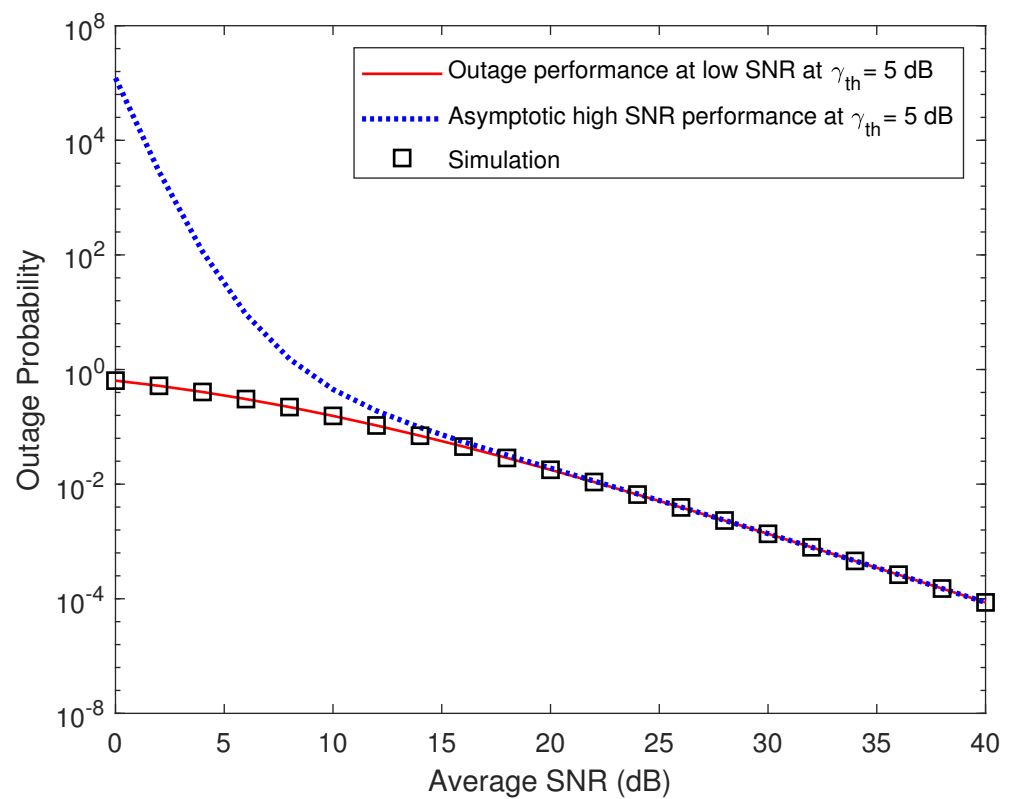


Figure 6. Outage probability of the system at high and low SNR regime.

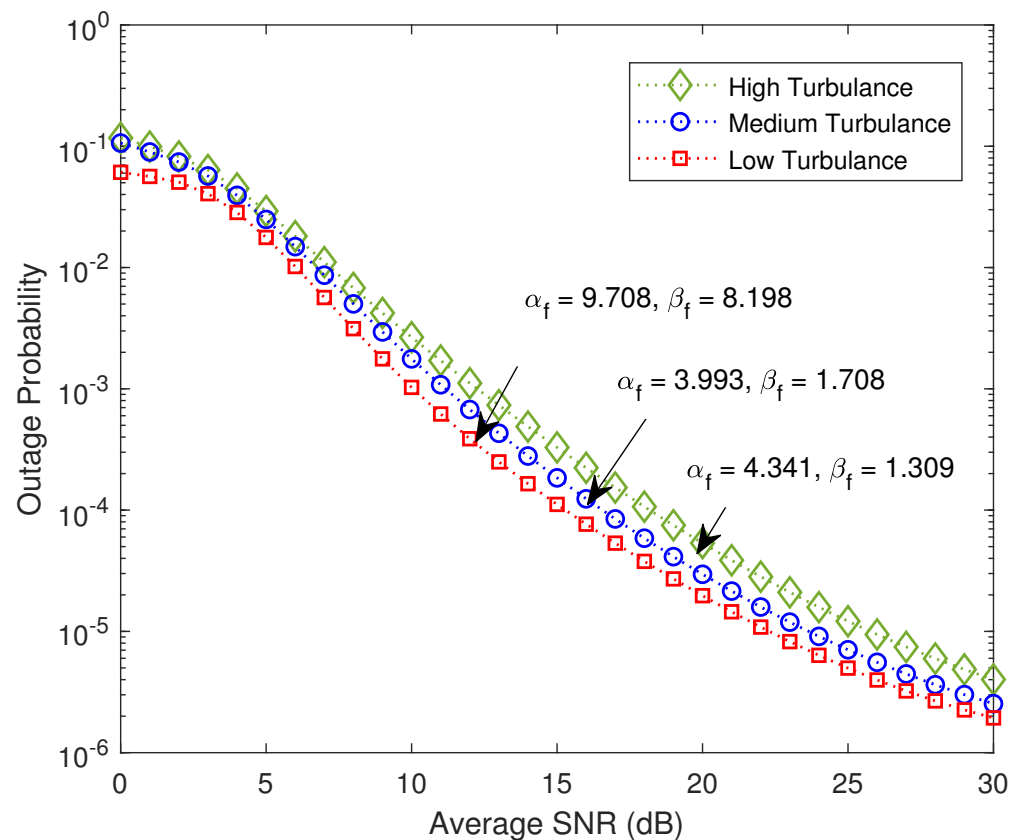


Figure 7. Outage probability of the system at various turbulent conditions.

6. Conclusions

In this paper, a UAV-based relay-assisted hybrid mixed RF/FSO/UWOC system has been proposed to maintain communication between two distant nodes, one above the terrestrial building and the other underwater. The analytical exact closed-form expressions for the outage probability of the system have been obtained using the CDF of the end-to-end SNR of the system. The outage performance of the system has also been analyzed at the high-SNR regime to gain insight into the system's performance. The derived theoretical expressions are verified using the simulation results, showing the effect of various system parameters such as atmospheric loss, pointing error, atmospheric turbulence, and link interruption due to angle of arrival and underwater turbulent parameters of the proposed system model's performance.

Author Contributions: Conceptualization, H.H.A. and N.K.S.; methodology, H.H.A. and R.M.A.Q.; software, A.M.M. and M.A.M.; validation, H.K. and P.S.; formal analysis, M.A. and A.V.; investigation, M.A.M.; resources, S.B. and R.M.A.Q.; data curation, H.K. and M.A.M.; writing—original draft preparation, A.M.M., A.V. and M.A.; writing—review and editing, H.K., P.K. and P.S.; visualization, S.B. and P.K.; supervision, N.K.S. and A.V.; project administration, M.A. and H.K.; funding acquisition, H.H.A. and N.K.S. All authors have read and agreed to the published version of the manuscript.

Funding: The authors extend their appreciation to the Deanship of Scientific Research at King Khalid University for funding this work through the Large Group Research Project under grant number RGP2/39/44.

Institutional Review Board Statement: Not applicable.

Informed Consent Statement: Not applicable.

Data Availability Statement: Not applicable.

Conflicts of Interest: The authors declare no conflict of interest.

References

1. Soleimani-Nasab, E.; Uysal, M. Generalized Performance Analysis of Mixed RF/FSO Cooperative Systems. *IEEE Trans. Wirel. Commun.* **2016**, *15*, 714–727. [[CrossRef](#)]
2. Al-Habash, A.; Andrews, L.C.; Philips, R.L. Mathematical model for the irradiance PDF of a laser beam propagating through turbulent media. *Opt. Eng. J.* **2001**, *40*, 1554–1562. [[CrossRef](#)]
3. Khalighi, M.A.; Uysal, M. Survey on Free Space Optical Communication: A Communication Theory Perspective. *IEEE Commun. Surv. Tutorials* **2014**, *16*, 2231–2258. [[CrossRef](#)]
4. Aggarwal, M.; Garg, P.; Puri, P. Analysis of subcarrier intensity modulation-based optical wireless DF relaying over turbulence channels with path loss and pointing error impairments. *IET Commun.* **2014**, *8*, 3170–3178. [[CrossRef](#)]
5. Vats, A.; Aggarwal, M.; Ahuja, S. End-to-End Performance Analysis of Hybrid VLC-RF System using Decode and Forward Relay in E-Health Medical Applications. *Opt.-Int. J. Electron Opt.* **2019**, *187*, 297–310. [[CrossRef](#)]
6. Khanna, H.; Aggarwal, M.; Ahuja, S. Performance analysis of a variable-gain amplify-and-forward relayed mixed RF-FSO system. *Int. J. Commun. Syst.* **2018**, *31*, e3400.
7. Puri, P.; Garg, P.; Aggarwal, M.; Sharma, P.K. Multiple user pair scheduling in bi-directional single relay assisted FSO systems. In Proceedings of the 2014 IEEE International Conference on Communications (ICC), Sydney, Australia, 10–14 June 2014; pp. 3401–3405.
8. Bag, B.; Das, A.; Ansari, I.S.; Prokes, A.; Bose, C.; Chandra, A. Performance Analysis of Hybrid FSO Systems Using FSO/RF-FSO Link Adaptation. *IEEE Photonics J.* **2018**, *10*, 7904417. [[CrossRef](#)]
9. Lee, E.; Park, J.; Han, D.; Yoon, G. Performance Analysis of the Asymmetric Dual-Hop Relay Transmission With Mixed RF/FSO Links. *IEEE Photonics Technol. Lett.* **2011**, *23*, 1642–1644. [[CrossRef](#)]
10. Shukla, N.K.; Mayet, A.M.; Vats, A.; Aggarwal, M.; Raja, R.K.; Verma, R.; Muqet, M.A. High speed integrated RF-VLC data communication system: Performance constraints and capacity considerations. *Phys. Commun.* **2022**, *50*, 101492. [[CrossRef](#)]
11. Zedini, E.; Ansari, I.; Alouini, M.-S. Performance analysis of mixed Nakagami-m and gamma-gamma dual-hop FSO transmission systems. *IEEE Photonics J.* **2015**, *7*, 1–20. [[CrossRef](#)]
12. Ansari, I.S.; Yilmaz, F.; Alouini, M. Impact of Pointing Errors on the Performance of Mixed RF/FSO Dual-Hop Transmission Systems. *IEEE Wirel. Commun. Lett.* **2013**, *2*, 351–354. [[CrossRef](#)]
13. Zedini, E.; Ansari, I.S.; Alouini, M. Unified performance analysis of mixed line of sight RF-FSO fixed gain dual-hop transmission systems. In Proceedings of the IEEE Wireless Communications and Networking Conference (WCNC), New Orleans, LA, USA, 9–12 March 2015; pp. 46–51.
14. Miridakis, N.I.; Matthaiou, M.; Karagiannidis, G.K. Multiuser Relaying over Mixed RF/FSO Links. *IEEE Trans. Commun.* **2014**, *62*, 1634–1645. [[CrossRef](#)]
15. Anees, S.; Bhatnagar, M.R. Performance evaluation of decode-and-forward dual-hop asymmetric radio frequency free space optical communication system. *IET Optoelectron.* **2015**, *9*, 232–240. [[CrossRef](#)]
16. Miridakis, N.I.; Matthaiou, M.; Karagiannidis, G.K. Multiuser dual-hop relaying over mixed RF/FSO links. In Proceedings of the IEEE International Conference on Communications (ICC), Sydney, NSW, Australia, 10–14 June 2014; pp. 3389–3394.
17. Yang, L.; Yuan, J.; Liu, X.; Hasna, M.O. On the Performance of LAP-Based Multiple-Hop RF/FSO Systems. *IEEE Trans. Aerosp. Electron. Syst.* **2019**, *55*, 499–505. [[CrossRef](#)]
18. Mamaghani, M.T.; Hong, Y. On the Performance of Low-Altitude UAV-Enabled Secure AF Relaying With Cooperative Jamming and SWIPT. *IEEE Access* **2019**, *7*, 153060–153073. [[CrossRef](#)]
19. Hanson, F.; Radic, S. High bandwidth underwater optical communication. *Appl. Opt.* **2008**, *47*, 277–283. [[CrossRef](#)] [[PubMed](#)]
20. Li, S.; Yang, L.; Costa, D. Performance Analysis of UAV-based Mixed RF/UWOC Transmission Systems. *arXiv* **2020**, arXiv:2011.09062.
21. Anees, S.; Deka, R. On the Performance of DF Based Dual-Hop Mixed RF/UWOC System. In Proceedings of the IEEE 89th Vehicular Technology Conference (VTC2019-Spring), Kuala Lumpur, Malaysia, 28 April–1 May 2019; pp. 1–5.
22. Yadav, S.; Vats, A.; Aggarwal, M.; Ahuja, S. Performance Analysis and Altitude Optimization of UAV-Enabled Dual-Hop Mixed RF-UWOC System. *IEEE Trans. Veh. Technol.* **2021**, *70*, 12651–12661. [[CrossRef](#)]
23. Anees, S.; Bhatnagar, M.R. Performance of an Amplify-and-Forward Dual-Hop Asymmetric RF-FSO Communication System. *IEEE Osa J. Opt. Commun. Netw.* **2015**, *7*, 124–135. [[CrossRef](#)]
24. Lei, H.; Zhang, Y.; Park, K.; Ansari, I.S.; Pan, G.; Alouini, M. On the Performance of Dual-Hop RF-UWOC System. In Proceedings of the IEEE International Conference on Communications Workshops (ICC Workshops), Dublin, Ireland, 7–11 June 2020; pp. 1–6.
25. Illi, E.; El Bouanani, F.; da Costa, D.B.; Sofotasios, P.C.; Ayoub, F.; Mezher, K.; Muhaidat, S. Physical Layer Security of a Dual-Hop Regenerative Mixed RF/UOW System. *IEEE Trans. Sustain. Comput.* **2021**, *6*, 90–104. [[CrossRef](#)]
26. Sarma, P.; Deka, R.; Anees, S. Performance Analysis of DF based Mixed Triple Hop RF-FSO-UWOC Cooperative System. In Proceedings of the IEEE 92nd Vehicular Technology Conference (VTC2020-Fall), Victoria, BC, Canada, 18 November–16 December 2020; pp. 1–5.
27. Alouini, M.; Simon, M.K. Performance of coherent receivers with hybrid SC/MRC over Nakagami-m fading channels. *IEEE Trans. Veh. Technol.* **1999**, *48*, 1155–1164. [[CrossRef](#)]
28. Shen, T.; Ochiai, H. A UAV-Enabled Wireless Powered Sensor Network Based on NOMA and Cooperative Relaying with Altitude Optimization. *IEEE Open J. Commun. Soc.* **2021**, *2*, 21–34. [[CrossRef](#)]

29. Aggarwal, M.; Garg, P.; Puri, P. Exact MGF-Based Performance Analysis of Dual-Hop AF-Relayed Optical Wireless Communication Systems. *J. Light. Technol.* **2015**, *33*, 1913–1919. [[CrossRef](#)]
30. Vaiopoulos, N.; Vavoulas, A.; Sandalidis, H.G. An assessment of a unmanned aerial vehicle-based broadcast scenario assuming random terrestrial user locations. *IET Optoelectron.* **2021**, *15*, 121–130. [[CrossRef](#)]
31. Safi, H.; Dargahi, A.; Cheng, J.; Safari, M. Analytical Channel Model and Link Design Optimization for Ground-to-HAP Free-Space Optical Communications. *J. Light. Technol.* **2020**, *38*, 5036–5047. [[CrossRef](#)]
32. The Mathematical Functions Site. Available online: <http://functions.wolfram.com> (accessed on 5 June 2022).
33. Zedini, E.; Oubei, H.M.; Kammoun, A.; Hamdi, M.; Ooi, B.S.; Alouini, M. Unified Statistical Channel Model for Turbulence-Induced Fading in Underwater Wireless Optical Communication Systems. *IEEE Trans. Commun.* **2019**, *67*, 2893–2907. [[CrossRef](#)]
34. Laneman, J.N.; Tse, D.N.C.; Wornell, G.W. Cooperative diversity in wireless networks: Efficient protocols and outage behavior. *IEEE Trans. Inf. Theory* **2004**, *50*, 3062–3080. [[CrossRef](#)]
35. Ikki, S.S.; Aissa, S. A Study of Optimization Problem for Amplify-and-Forward Relaying over Weibull Fading Channels with Multiple Antennas. *IEEE Commun. Lett.* **2011**, *15*, 1148–1151. [[CrossRef](#)]
36. Vats, A.; Aggarwal, M.; Ahuja, S. Outage and error analysis of three hop hybrid VLC/FSO/VLC-based relayed optical wireless communication system. *Trans. Emerg. Telecommun. Tech.* **2019**, *30*, e3544. [[CrossRef](#)]
37. Zhong, C.; Wong, K.; Jin, S.; Alouini, M.; Ratnarajah, T. Asymptotic Analysis for Nakagami-m Fading Channels with Relay Selection. In Proceedings of the IEEE International Conference on Communications (ICC), Kyoto, Japan, 5–9 June 2011; pp. 1–5.
38. Dale, M. *The Algebra of Random Variables*; Wiley: New York, NY, USA, 1979; Volume 1.
39. Amer, M.; Al-Eryani, Y. Underwater optical communication system relayed by $\alpha - \mu$ fading channel: Outage, capacity and asymptotic analysis. *arXiv* **2019**, arXiv:1911.04243.

Disclaimer/Publisher’s Note: The statements, opinions and data contained in all publications are solely those of the individual author(s) and contributor(s) and not of MDPI and/or the editor(s). MDPI and/or the editor(s) disclaim responsibility for any injury to people or property resulting from any ideas, methods, instructions or products referred to in the content.